# 5. Near-Infrared Science

The WFC3 infrared channel has unique and powerful capabilities in the 0.8-1.7 μm spectral region. HST, even with a relatively warm optical system, offers four key advantages for near IR imaging over much larger ground-based facilities:

- continuous coverage of the 0.8-1.7 μm wavelength range, unaffected by the atmospheric water vapor absorption which mutilates ground-based data;

- a reduction by nearly 3 orders of magnitude in the sky background emission shortwards of 1.7 μm (due primarily to atmospheric OH bands);

- the ability to have stable, uniform, near diffraction-limited imaging over a large field of view ($135 \times 135$ arcsec with WFC3);

- stable and accurate photometry over a large field of view compared to the small isoplanatic patch and variable point spread function available to ground-based adaptive optics (AO) systems.

Such a potent combination of performance characteristics is impossible to achieve from the ground and makes the near-IR capabilities of WFC3 compelling.

In the design of WFC3/IR it was decided not to cover wavelengths out to the 2.5 μm cutoff of NICMOS. This compromise allows the WFC3 near-IR detector to be cooled simply by thermo-electric coolers, rather than by expendable cryogen or a mechanical cooler. The fact that WFC3-IR does not extend to the K band (2.2 μm) is not a serious limitation, since the HST Optical Telescope Assembly (OTA) itself generates a significant background at K, while adaptive-optics systems on large ground-based telescopes optimized for IR performance will become very competitive in the K band during this decade. On the other hand, the reduction in the H band (1.6 μm) sky background in space renders HST near-IR imagers more sensitive than similar instruments on 8-meter class ground-based telescopes, even with sophisticated adaptive-optics systems. Thanks to the use of more modern detectors, WFC3 improves on the discovery efficiency of NICMOS by more than a factor of 15. Below we have singled out a few examples from the many programs that are made possible by WFC3/IR.

# 5.1 The Highest -Redshift Galaxies

Deep observations with HST and ground-based telescopes demonstrate that there are hundreds of thousands of faint, distant galaxies per square degree of sky. Because spectroscopic integration times are long, even for ground-based telescopes in the 8-m to 10-m class, it is essential to employ efficient survey techniques that can isolate the objects of greatest interest for various astrophysical investigations. As we have already discussed, the most productive technique for identifying high-redshift, star-forming galaxies is the "Lyman-dropout" method, which at low redshift relies on the Lyman discontinuity at 912 Å. As the redshift increases, the effect of absorption due to intergalactic neutral hydrogen clouds – known as the *Lyman-$\alpha$ forest* - moves the rest-frame wavelength of the continuum drop from the Lyman limit at 912 Å up to the Lyman $\alpha$ at 1216 Å. Both discontinuities can be detected readily in multiband imaging. This method has been used with both ground-based and HST imaging to identify candidate galaxies in the $z \sim 3$-5 redshift range, and will most likely be the technique for providing us with the first large samples of objects beyond redshift 5. WFC3/IR can open new territory to this method, and - thanks to its sensitivity and field of view - achieve real breakthroughs in the search for the highest-redshift galaxies. In particular, a problem that WFC3/IR can tackle is that of constraining the so-called re-ionization epoch of the Universe. This is the time when the neutral gas permeating the Universe since the release of the cosmic microwave background - at redshift above 1000 - becomes ionized again and thus transparent to Lyman-$\alpha$ light. According to some recent models, this epoch, known to cosmologists as the *End of the Dark Ages*, should occur at a redshift between 6 and 10. For galaxies at redshift 7 through 10 the Lyman break will occur at 1-1.3 $\mu$m and appear as I or J band dropouts (see Figure 8). They will be identified by deep I, J, and H band deep observations. Since the search must be carried out with high sensitivity over a wide field in the near-IR and because high-redshift galaxies are generally very compact (<0.2 arcsec in size), ground-based facilities will not be competitive with WFC3/IR for this particular project. WFC3/IR will be in a position to verify the model predictions and, if they are correct, to see the first objects shining through the Universe. Depending on their nature, WFC3/IR may even detect the objects responsible for the re-ionization itself.

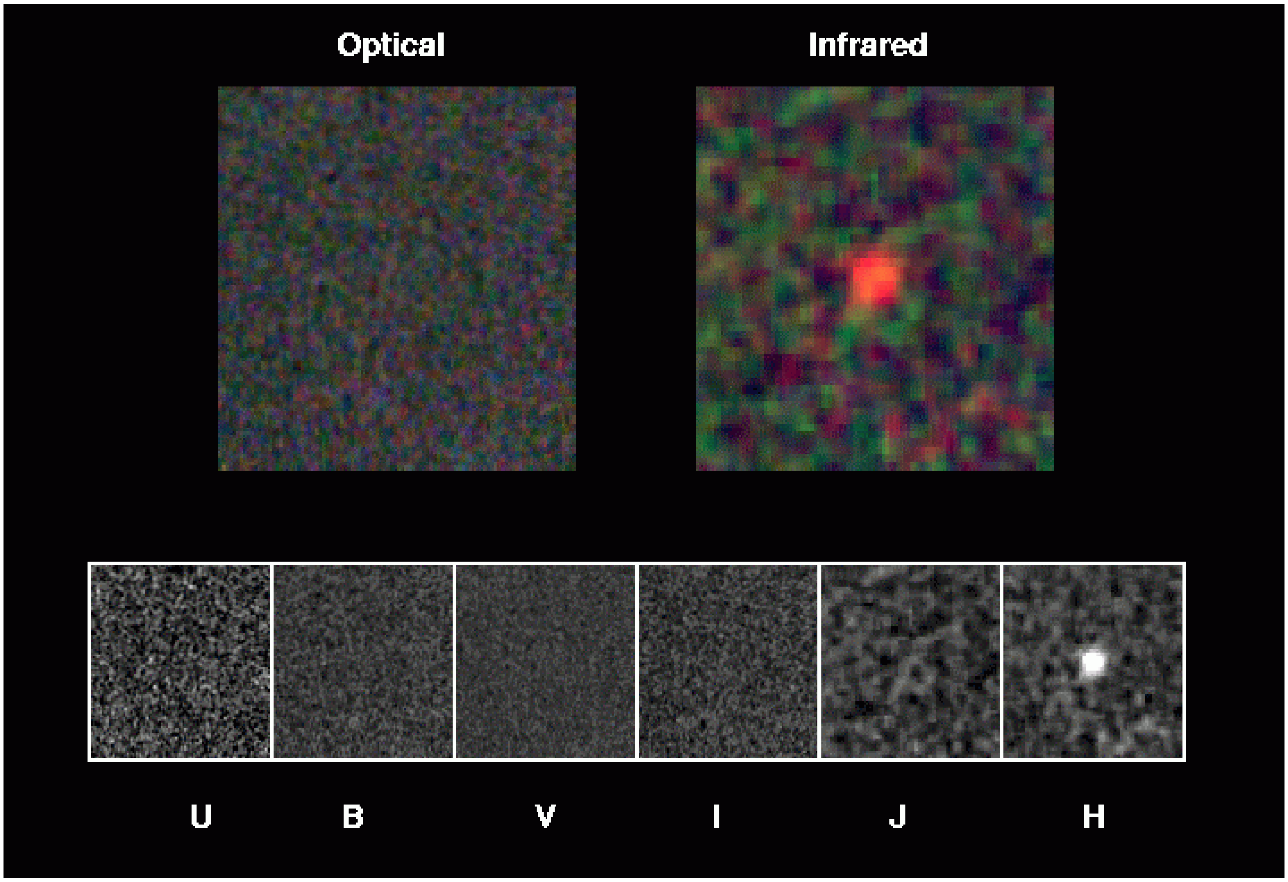


Figure 8. J-dropout object identified in the Hubble Deep Field North. This object is visible only in the NICMOS F160W (H) image. The U, B, V, and I images were obtained with WFPC2, the J and H images with NICMOS. Similar objects could be found in large numbers by WFC3 by searching a large area for sources bright in the H band and faint in the J band (M. Dickinson).

## 5.2 Water and Ices on Mars and the Outer Planetary Satellites

Despite three and a half decades of Mars exploration, a great deal of uncertainty remains over the amount, disposition, and variability of water vapor in the planet's atmosphere and its relation to subsurface ice, hydrated minerals, and other volatiles. WFC3 offers the prospect to measure Mars' atmospheric water vapor with spatial resolution down to a few tens of km with a filter designed for the 1.4 μm water-vapor band (see Figure 9). The spatial resolution and sensitivity to small spatial and temporal changes in water vapor measured in this way exceeds the capabilities of ground-based telescopes by a wide margin. Given the requirements on spatial resolution, minimal scattered light, and the fact that 1.4 μm is in the center of the Earth's atmospheric water band, observations such as these are possible only from space. Observations with HST complement *in situ* measurements with spacecraft since the latter can only carry out local measurements and are less well suited to follow seasonal variations in the Martian atmosphere water vapor content.

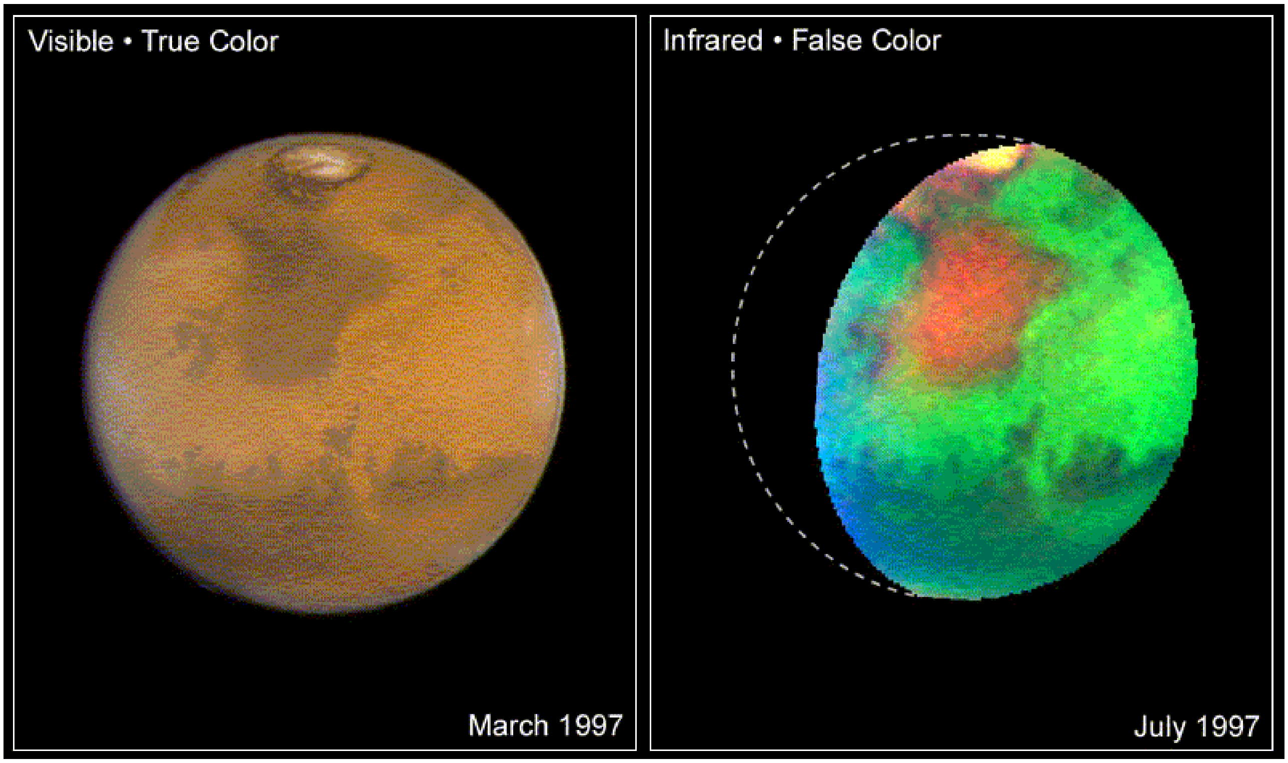


Figure 9. Water in Martian rocks as revealed by WFPC2 (left panel) and NICMOS (right panel) observations. The bluer shade along the edges of the Martian disk in the left panel is due to atmospheric haze and water ice clouds. The large reddish region in the right panel identifies an area of water-rich minerals known as Mare Acidalium (J. Bell, J. Maki, M. Wolff, and NASA).

The surfaces of many of the satellites of the outer solar system planets have long been known to retain ice. Because temperature declines with distance from the Sun, the dominant type of ice varies with solar distance, from $H_2O$ in the satellites of Jupiter and Saturn, to $CH_4$ (Uranus) and CO and $N_2$ (Neptune's Triton). It is likely that additional ices await discovery on the surfaces of satellites from Jupiter to Neptune, and there is a possibility for major surprises. The most spectrally active ices, for example, are not necessarily the most abundant ices. Methane on Pluto was once thought to be a dominant constituent, but is now recognized to be only a small contaminant of nitrogen, the truly dominant constituent. Ground-based data suffer from inadequate signal-to-noise ratio and from errors due to subtraction of the scattered-light background from the adjacent planets. This is especially true of the faint, inner satellites (e.g. JV, JXIV, S15, U7) for which no suitable near-IR spectra exist. The low scattered-light background of HST will allow the first high-quality near infrared (slitless) spectra of many planetary satellites. Of particular value will be WFC3's continuous coverage from 0.8 to 1.7 μm.